International Journal of Pharmaceutics 424 (2012) 98–106

Contents lists available at SciVerse ScienceDirect

International Journal of Pharmaceutics

journal homepage: www.elsevier.com/locate/ijpharm

Pharmaceutical nanotechnology

A comparison between spray drying and spray freeze drying for dry powder inhaler formulation of drug-loaded lipid–polymer hybrid nanoparticles

Yajie Wang[1], Katherine Kho[1], Wean Sin Cheow, Kunn Hadinoto*

School of Chemical and Biomedical Engineering, Nanyang Technological University, Singapore 637459, Singapore

ARTICLE INFO

Article history:
Received 15 September 2011
Received in revised form 8 December 2011
Accepted 25 December 2011
Available online 31 December 2011

Keywords:
Spray drying
Spray freeze drying
Hybrid nanoparticles
Dry powder inhaler
Leucine

ABSTRACT

Lipid–polymer hybrid nanoparticles – polymeric nanoparticles enveloped by lipid layers – have emerged as a potent therapeutic nano-carrier alternative to liposomes and polymeric nanoparticles. Herein we perform comparative studies of employing spray drying (SD) and spray freeze drying (SFD) to produce inhalable dry-powder form of drug-loaded lipid–polymer hybrid nanoparticles. Poly(lactic-co-glycolic acid), lecithin, and levofloxacin are employed as the polymer, lipid, and drug models, respectively. The hybrid nanoparticles are transformed into micro-scale nanoparticle aggregates (or nano-aggregates) via SD and SFD, where the effects of (1) different excipients (i.e. mannitol, polyvinyl alcohol (PVA), and leucine), and (2) nanoparticle to excipient ratio on nano-aggregate characteristics (e.g. size, flowability, aqueous reconstitution, aerosolization efficiency) are examined. In both methods, PVA is found more effective than mannitol for aqueous reconstitution, whereas hydrophobic leucineis needed to achieve effective aerosolization as it reduces nano-aggregate agglomeration. Using PVA, both methods are equally capable of producing nano-aggregates having size, density, flowability, yield and reconstitutibility in the range ideal for inhaled delivery. Nevertheless, nano-aggregates produced by SFD are superior to SD in terms of their aerosolization efficiency manifested in the higher emitted dose and fine particle fraction with lower mass median aerodynamic diameter.

1. Introduction

Pulmonary delivery of therapeutic nanoparticles has recently gained significant interests because of its bioavailability enhancement potential attributed to the unique ability of nanoparticles to evade the lung phagocytic and mucociliary clearance mechanisms resulting in prolonged drug residence time (Rogueda and Traini, 2007). A majority of studies on inhaled therapeutic nanoparticles employ polymeric nano-carriers, in particular poly(lactic-co-glycolic acid) (PLGA), owed to its well-established biocompatibility and biodegradability. Specific to dry powder inhaler (DPI), the extensive use of PLGA nanoparticles as carriers are even more evident.

Nomenclature

ρ_{bulk}	bulk density (g/cm^3)
ρ_{eff}	effective density (g/cm^3)
ρ_S	unit density (1 g/cm^3)
ρ_{tap}	tap density (g/cm^3)
d_A	measured aerodynamic diameter from cascade impactor (μm)
$d_{A,\,theory}$	theoretical aerodynamic diameter calculated from Eq. (1) (μm)
d_G	geometric diameter (μm)
S_f	nanoparticle size after aggregate reconstitution (nm)
S_i	raw nanoparticle size before SD or SFD (nm)
T_g	glass transition temperature (°C)

Unlike other biocompatible and biodegradable polymers (e.g. polycaprolactone), PLGA nanoparticles are structurally robust and thermally insensitive, such that they can be transformed from the aqueous suspension form into inhalable dry powders by spray drying, without the need of rigorous formulation steps other than inclusion of drying adjuvants, while preserving their physicochemical characteristics (e.g. size, drug loading). A number of DPI

Abbreviations: CI, cohesion index; DCM, dichloromethane; DPI, dry powder inhaler; ED, emitted dose; FPF, fine particle fraction; GRAS, generally recognized as safe; IP, induction port; LC, lecithin; LEU, leucine; MMAD, mass median aerodynamic diameter; NGI, next generation impactor; NP, nanoparticles; PCS, photon correlation spectroscopy; PDT, powder dispatchment tube; PLGA, poly(lactic-co-glycolic acid); PS, pre-separator; PVA, polyvinyl alcohol; SD, spray drying; SEM, scanning electron microscope; SFD, spray freeze drying.

* Corresponding author. Tel.: +65 6514 8381; fax: +65 6794 7553.
E-mail address: kunnong@ntu.edu.sg (K. Hadinoto).

[1] These authors contributed equally to this work.

0378-5173/$ – see front matter © 2012 Elsevier B.V. All rights reserved.
doi:10.1016/j.ijpharm.2011.12.045

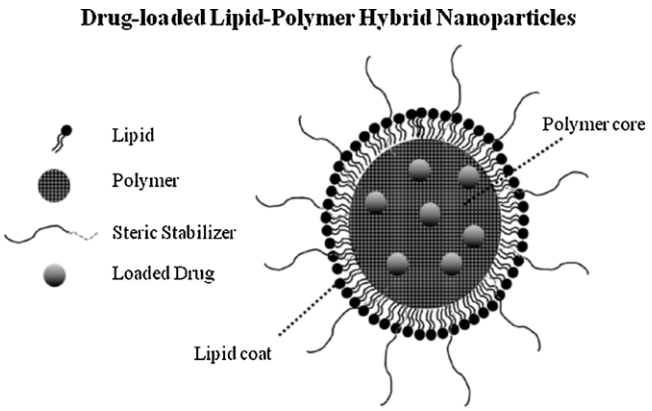

Fig. 1. Illustration of drug-loaded lipid–polymer hybrid nanoparticles.

formulations of spray-dried PLGA nanoparticles in the form of micro-scale spherical aggregates of the nanoparticles have been presented for various therapeutic functions ranging from drug (Ohashi et al., 2009; Sung et al., 2009; Tomoda et al., 2009) to gene (Jensen et al., 2010; Takashima et al., 2007) deliveries.

Recently, a new class of therapeutic nano-carriers known as lipid–polymer hybrid nanoparticles has emerged as a potentially more potent alternative to polymeric nanoparticles. Lipid–polymer hybrid nanoparticles are polymeric nanoparticles enveloped by lipid layers (Fig. 1), which combine the main beneficial characteristics of liposomal drug delivery – cell affinity and cell targeting ability – with those of polymeric nanoparticles – structural integrity, controlled release, and ease of functionalization to achieve high serum stability (Zhang et al., 2008). Furthermore, hybrid nanoparticles are generally more hydrophobic than surfactant-stabilized polymeric nanoparticles resulting in increased cell uptake and lower cytotoxicity (Su et al., 2011). In addition, the inclusion of lipid coat enables the hybrid nanoparticles to encapsulate not only water-insoluble drugs, but also water-soluble drugs with greater encapsulation efficiency (Cheow and Hadinoto, 2011).

Unsurprisingly, PLGA has been the most widely used polymer for the hybrid nanoparticle formulation (Bershteyn et al., 2008; Cheow and Hadinoto, 2011; Hu et al., 2010; Zheng et al., 2010). Hybrid PLGA nanoparticles are typically prepared by a modified emulsification method, similar to that employed in the non-hybrid PLGA nanoparticle preparation. Whereas polyvinyl alcohol (PVA) is used as the surfactant stabilizer in non-hybrid PLGA nanoparticles owed to its high biocompatibility, both natural and synthetic phospholipids are used, in place of PVA, to prepare hybrid PLGA nanoparticles.

Herein we investigate the feasibility of creating DPI formulation of lipid–polymer hybrid nanoparticles containing PLGA and lecithin (LC) as the polymer and lipid constituents, respectively. Lecithin is a component of cell membranes and has been incorporated into various pharmaceutical products, mostly as an emulsifying or solubilizing agent in intramuscular and intravenous injectables (Wade and Weller, 1994). Instead of the conventional DPI formulation, which employs coarse inert particles as the carriers of drug-bearing particles, we aim to formulate the PLGA–LC nanoparticles into micro-scale nanoparticle aggregate (or nano-aggregate) structures for carrier-free DPI delivery. The nano-aggregates possess large geometric size (d_G) and low density (ρ_{eff}) resulting in theoretical aerodynamic diameter ($d_{A,\,theory}$ in Eq. (1)) between 1 and 5 μm ideal for pulmonary delivery. The large d_G (>5 μm) of the nano-aggregates make them readily aerosolized off the inhaler without the need of coarse carrier particles, while remain effectively deposit in the lung owed to the small $d_{A,\,theory}$ (Sung et al., 2009).

$$d_{A,\ \text{theory}} = d_G\sqrt{\frac{\rho_{eff}}{\rho_S}} \quad \text{where } \rho_S = 1\,\text{g/cm}^3 \tag{1}$$

In addition to the aerosolization and lung deposition efficiency, another important characteristic of the nano-aggregates is their ability to reconstitute back into individual nanoparticles once they deposit in the aqueous environment of the airway lumen. Nano-aggregate reconstitutibility is crucial for the nanoparticles to evade the lung clearance mechanisms, therefore maintaining their therapeutic functions. To ensure nano-aggregate reconstitution, Generally Recognized as Safe (GRAS) excipients (e.g. lactose, leucine) are typically included in the spray drying process, where the roles of the excipients are as (1) drying adjuvants that protect the structural integrity of the polymeric nanoparticles upon exposure to high temperature and (2) "interstitial bridges" that occupy the interstitial space between the nanoparticles, hence preventing the polymeric nanoparticles from forming irreversible interparticle fusion upon heating above their glass transition temperature.

In an aqueous environment, the "interstitial bridges" would dissolve, therefore releasing the nanoparticles from the aggregate network. The extent of the reconstitution depends on the hydrophilicity of the excipients. Unlike spray-dried PLGA–PVA nano-aggregates, which readily disassociate in water even when poorly water-soluble leucine (≈25 mg/mL) is used as the excipient, our preliminary results on spray drying of hybrid PLGA–LC nanoparticles, using highly water soluble mannitol (≈180 mg/mL) as the excipient, indicate poorly reconstituted nano-aggregates. Adding leucine does improve the nano-aggregate reconstitution to a certain extent, however, it fails to fully reconstitute the nano-aggregates into individual nanoparticles. For brevity, the results of our preliminary experiments are not presented here, but in the Supplementary Data (Table S1).

The poor reconstitutibility of the PLGA–LC hybrid nano-aggregates is thought to be caused by lecithin being in its wax-like phase at temperature above 40 °C (Small, 1967). It is believed that following the nano-aggregate formation, the wax-like lecithin present on the nanoparticle surface causes inter-nanoparticle fusions within the aggregates. As the temperature decreases from 40 °C to 45 °C in the spray-dryer outlet to room temperature in the powder collection vessel, the inter-nanoparticle fusions become permanent as lecithin transform into its partially crystalline powder state at temperature below 40 °C (Small, 1967). In addition to the poor reconstitution, the PLGA–LC nano-aggregates are highly cohesive due to the hygroscopic nature of both mannitol and lecithin resulting in low spray drying yield and extremely poor aerosolization off the inhaler. Therefore, DPI formulation of hybrid nanoparticles having better nano-aggregate constitution and aerosolization efficiency is pursued here.

First, we investigate the use of PVA as the spray-drying excipient in place of mannitol, where we postulate that the presence of PVA will minimize inter-nanoparticle fusions as our earlier study (Cheow et al., 2011) has demonstrated that PVA coats polymeric nanoparticle surfaces upon its precipitation. Furthermore, spray drying of drug solution with PVA has been found to produce particles with low moisture content, despite the high hydrophilicity of PVA, resulting in effective aerosolization (Salama et al., 2008). Second, recognizing the adverse effect of high-temperature drying on the hybrid nano-aggregate reconstitution, we explore the feasibility of employing a low-temperature drying process (i.e. spray freeze drying) to produce inhalable PLGA–LC nano-aggregates. The spray-freeze-dried and spray-dried nano-aggregates are examined in terms of their morphology, production yield, flowability, aqueous reconstitution, and aerosolization efficiency. Antibiotic

levofloxacin is loaded into the nanoparticles to create a model for drug-loaded lipid–polymer hybrid nanoparticles. Mannitol and PVA are used as hydrophilic excipients, and leucine as hydrophobic excipient.

2. Materials and methods

2.1. Materials

PLGA 50:50 Purasorb 5004A is a gift from Purac Biomaterials (Netherlands). D-Mannitol, L-leucine (LEU), soy-bean lecithin (LC), PVA (MW = 13–23,000), levofloxacin, and dichloromethane (DCM) are all purchased from Sigma–Aldrich (USA).

2.2. Methods

2.2.1. Lipid–polymer hybrid nanoparticle preparation and characterization

The hybrid PLGA–LC nanoparticles are prepared by a $w_1/o/w_2$ double-emulsification-solvent-evaporation method. Briefly, 30 mg LC and 90 mg PLGA are dissolved in 3 mL DCM to form the oil phase, while 9 mg of the drug is dissolved in 300 μL deionized water to form the internal aqueous phase (w_1). Next, the aqueous drug solution is emulsified in the PLGA organic solution by sonication for 60 s. The resultant nano-emulsion is poured into 12 mL deionized water (w_2) and is sonicated again for 60 s. Afterwards, the nano-emulsion is stirred overnight at room temperature to evaporate off DCM, and the resultant nanoparticle suspension is centrifuged twice at 11,000 rpm to remove the non-encapsulated drug and excess LC.

The size and zeta potential of the hybrid nanoparticles are measured by photon correlation spectroscopy (PCS) using Brookhaven 90Plus Nanoparticle Size Analyzer (Brookhaven Instruments Corporation, USA). Steric stabilizer is not included in the current formulation as the nanoparticles produced are already stable. The drug encapsulation efficiency is determined from the ratio of the encapsulated drug to the drug initially added. The encapsulated drug is determined by subtracting the drug present in the supernatant after centrifugation from the drug initially added. The drug concentration in the supernatant is measured by UV-VIS spectrophotometer (UV Mini-1240, Shimadzu, Japan) at 254 nm. The drug loading is determined from the ratio of the encapsulated drug to the total nanoparticle mass.

2.2.2. Spray drying of lipid–polymer hybrid nanoparticles

BUCHI B-290 mini spray dryer (BÜCHI, Switzerland) is employed in the spray-drying (SD) experiment using a two-fluid atomizer with a nozzle diameter of 1.5 mm. The feed and atomizing gas flow rates are fixed at 0.18 L/h and 333 L/h, respectively. The total solid concentration (i.e. nanoparticles + excipient) in the feed is maintained at 1.0% (w/v). The ratio of nanoparticle to excipient in the feed is varied from 80% to 50% (w/w) nanoparticle content. 10% (v/v) aqueous ethanol solution with boiling point equal to 92 °C is used as the SD medium. The lower boiling point enables the production of sufficiently dry products at a lower inlet temperature (i.e. 80 °C), than that required when water is used as the medium (i.e. 100 °C). The lower inlet temperature in turn leads to a lower outlet temperature around 40–45 °C hence minimizing the high-temperature exposure of LC. Furthermore, the outlet temperature is below the glass transition temperature of PLGA50:50 Purasorb 5004A ($T_g \approx 47$ °C) (D'Aurizio et al., 2011), therefore ensuring that structural integrity of the nanoparticles is preserved.

2.2.3. Spray freeze drying of lipid–polymer hybrid nanoparticles

In spray freeze drying (SFD), nano-aggregates are produced by atomizing the feed solution into liquid nitrogen followed by lyophilization of the frozen droplets after evaporating the liquid nitrogen. The SFD experiment is performed in a modified B-290 mini spray-dryer (Fig. 2A), where the drying chamber is removed and replaced with a polypropylene vessel containing 400 mL of liquid nitrogen under constant stirring at 500 rpm. The distance between the nozzle tip and liquid nitrogen surface is fixed at 10 cm. The total solid concentration in the feed is maintained at 2.5% (w/v). A higher feed concentration is needed in SFD compared to SD in order to obtain a reasonable production yield. Consequently, the feed and atomizing gas flow rates must be adjusted to 0.27 L/h and 410 L/h, respectively, in order to obtain nano-aggregates with the desired morphology (Kho and Hadinoto, 2011). Nanoparticle contents in the feed are varied between 50 and 60% (w/w). The frozen droplets are lyophilized at −52 °C and 0.05 mbar for 24 h in Alpha 1-2 LD Plus freeze dryer (Martin Christ, Germany).

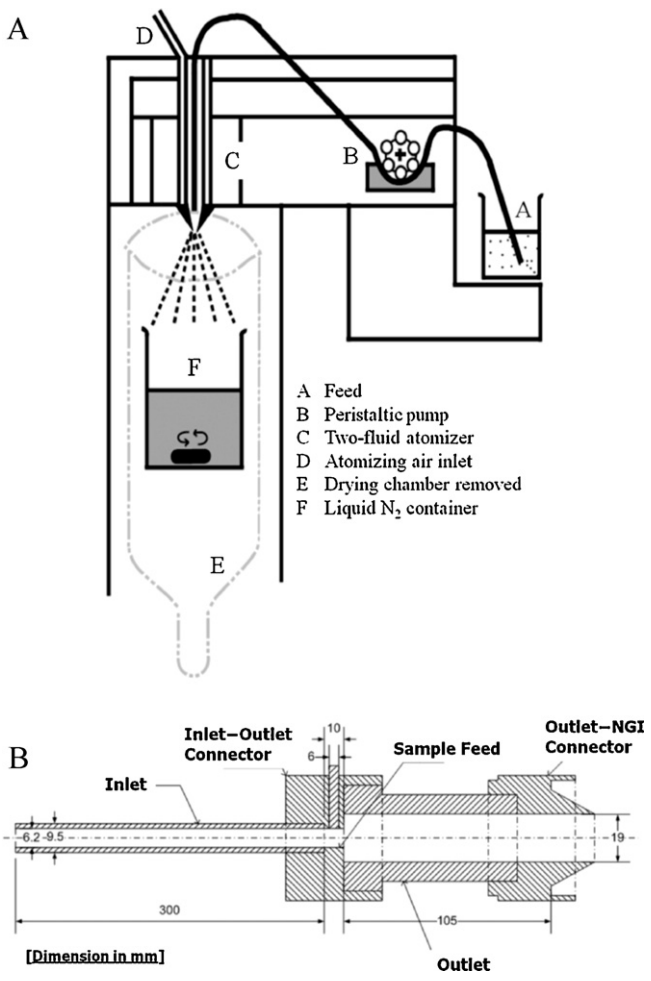

Fig. 2. Schematic diagrams of (A) SFD setup and (B) powder dispatchment tube (PDT).

2.2.4. Powder characterizations: morphology, production yield, and flowability

The SD and SFD powders are stored in a dry cabinet for 48 h prior to characterizations, which are performed with minimum of two replicates. The production yield is calculated from the mass ratio of the collected powders to the total solid in the feed. Nano-aggregate morphology is characterized by scanning electron microscope (SEM) JSM-6700F (JEOL, USA). The volume-averaged d_G is determined from 1000 particle counts of the SEM images using ImageJ software (NIH, USA). ρ_{eff} is determined from the tap density, ρ_{tap}, using a tap densitometer (Quantachromme, USA) after

2000 taps. $d_{A,\,theory}$ is calculated from Eq. (1) using experimental measurements of d_G and ρ_{eff}.

The powder flowability is characterized by Carr's index calculated from Eq. (2), where ρ_{bulk} is the bulk particle density determined by measuring the volume of powders of a known mass in a 5 mL measuring cylinder without tapping. The particles are categorized as free-flowing when Carr's index ≤25 and having poor-flowability when Carr's index ≥40. Experimental uncertainties in the characterization of d_G, ρ_{eff}, yield, and Carr's index are ±7%, 8%, 10%, and 7%, respectively. A *t*-test analysis ($\alpha = 0.05$) is performed to evaluate statistical significances of the mean values obtained from different experimental groups.

$$\text{Carr's index} = \left(1 - \frac{\rho_{bulk}}{\rho_{top}}\right) \times 100\% \quad (2)$$

2.2.5. Characterization of nano-aggregate reconstitution

Nano-aggregate reconstitution in an aqueous medium is characterized from the change in the nanoparticle size before and after reconstitution. S_f is the volume-averaged size of the nanoparticles recovered after reconstitution, whereas S_i is the volume-averaged raw nanoparticle size before SD or SFD (Kho and Hadinoto, 2010). S_f/S_i ratio ≈1 denotes complete reconstitution, whereas S_f/S_i ratio ≫1 denotes poor reconstitution. We select $S_f/S_i \leq 1.5$ as the demarcation for effective nano-aggregate reconstitution. Briefly, 10 mg of the nano-aggregates is added into 2 mL of deionized water under gentle stirring. The suspension is centrifuged at 6000 rpm for 10 min after which 1.5 mL of the supernatant is collected and S_f is measured by PCS. The nano-aggregate reconstitution characterization is performed in triplicates. The experimental uncertainty in S_f/S_i characterization is ±3%.

2.2.6. Characterization of nano-aggregate aerosolization efficiency

Four parameters, i.e. (1) emitted dose (ED), (2) fine particle fraction (FPF), (3) mass median aerodynamic diameter (MMAD), and (4) cohesion index (CI) are examined to characterize the nano-aggregate aerosolization efficiency. A seven-stage Next Generation Impactor (NGI, Copley Scientific, UK) equipped with an induction port (IP) and a pre-separator (PS) is used. ED is defined as the mass percentage of the powders that are successfully entrained off the inhaler and recovered in the NGI. FPF is defined as the mass percentage of the recovered powders with cut-off $d_A \leq 5$ μm, whereas MMAD is defined as the mass median d_A value of the recovered powders. CI is defined as the ratio of MMAD to $d_{A,\,theory}$, where high CI indicates strong agglomeration of the entrained nano-aggregates. Experimental uncertainties in the ED, FPF, MMAD, and CI characterizations are ±8%, 3%, 3%, and 11%, respectively, from a minimum of two replicates.

A powder dispatchment tube (PDT) is employed in place of an inhaler to enable the aerosolization efficiency to be examined independent of the inhaler type (Louey et al., 2006). The use of PDT has been validated using two commercial inhalers (i.e. inhalator and rotahaler) (Louey et al., 2006). The PDT consists of three sections, namely (i) the inlet, (ii) sample feed, and (iii) outlet connected to the IP of NGI (Fig. 2B). 5 mg of powders are placed in the sample feed section equipped with a removable mesh that functions as powder disperser. Using the critical flow controller (Copley Scientific, UK), the airflow rate is set at 85 L/min to ensure the recommended 4 kPa pressure drop in the PDT. The airflow duration is set at 2.8 s to mimic four liters of air drawn in human inhalation. The effective cut-off d_A for each stage at 85 L/min is 6.7, 3.7, 2.4, 1.4, 0.8, 0.5 and 0.3 μm for stages 1–7, respectively. The PS and stages are coated with silicone grease to prevent re-entrainment of the powders after deposition.

The amount of the recovered powders is quantified using colorimetric assay of the excipients, i.e. mannitol (Sanchez, 1998) and PVA (Finley, 1961). As both SD and SFD are based on suspension-to-droplet approach, the excipient content in the sprayed droplets, as well as in the dry powders, is proportional to the nanoparticle to excipient ratio in the feed. Therefore, by knowing the amount of excipient recovered from the dry powders, the amount of nano-aggregates deposited can be calculated based on the nanoparticle to excipient ratio in the feed.

For mannitol, the recovered powders are suspended in 2 mL deionized water to dissolve the mannitol. Next, the suspension is centrifuged at 14,000 rpm for 12 min. The supernatant is collected and diluted to 2 mL with deionized water. 1 mL of 5 mM sodium periodate is added to the supernatant and agitated for 15 s. Afterwards, 1 mL solution containing 0.1 M acetylacetone, 2 M ammonium acetate, and 0.02 M sodium thiosulfate is added and agitated for 15 s. The mixture is heated at 100 °C for 2 min followed by cooling in an ice bath. The mannitol absorbance is measured at 412 nm using UV-VIS spectrophotometer. For PVA, the same procedures up to the supernatant dilution step are employed. Next, 1.2 mL of 4% (w/v) boric acid solution, 0.24 mL of iodine solution – 1.27% (w/v) iodine in 2.5% (w/v) potassium iodide, and 0.56 mL of deionized water are added to the supernatant resulting in the formation of PVA–iodine complex. The PVA concentration is measured by UV-VIS spectrophotometer at 644 nm.

3. Results and discussion

3.1. Lipid–polymer hybrid nanoparticles

The volume-averaged size of the PLGA–LC nanoparticles is ≈420 ± 30 nm with zeta potential in the range of (–) 25–30 mV denoting their high colloidal stability. The drug is successfully encapsulated into the hybrid nanoparticles at ≈19% encapsulation efficiency resulting in drug loading ≈2.0% (w/w).

3.2. Spray-dried lipid–polymer hybrid nano-aggregates

The physical characteristics and aerosolization efficiency of the spray-dried PLGA–LC nano-aggregates using PVA as the excipient are presented in Tables 1 and 2, respectively. The reported values are the average of the replicates. The effect of the nanoparticle to excipient ratio is investigated first. At 80% (w/w) nanoparticle content in Run 0, nano-aggregates of very small d_G (<3 μm) and

Table 1
SD: nano-aggregate physical characteristics with PVA and leucine as the excipients.

Run	NP (%, w/w)	PVA (%, w/w)	LEU (%, w/w)	d_G (μm)	ρ_{eff} (g/cm^3)	$d_{A,\,theory}$ (μm)	Yield (%, w/w)	Carr's index	S_f/S_i
0	80	20	–	2.6	0.13	0.9	69	41	2.7
1.1	70	30	–	8.6	0.21	4.0	65	25	1.3
1.2		22	8	8.6	0.25	4.3	21	22	1.7
2.1	60	40	–	8.2	0.21	3.8	38	25	1.2
2.2		30	10	5.4	0.25	2.7	36	22	1.5
2.3		10	30	6.7	0.24	3.3	16	37	1.8
3.1	50	15	35	5.9	0.22	2.8	24	33	1.2
3.2		10	40	8.7	0.29	4.7	23	38	1.1

Table 2
SD: nano-aggregate aerosolization characteristics with PVA and leucine as the excipients.

Run	ED (%, w/w)	FPF (%, w/w)	MMAD (μm)	CI
1.1	<10	Poor aerosolization		
1.2				
2.1	<10	Poor aerosolization		
2.2	62	3	7.8	2.9
2.3	51	10	6.8	2.0
3.1	66	12	7.0	2.5
3.2	68	23	6.6	1.4

low ρ_{eff} (≈0.13 g/cm^3) are produced resulting in $d_{A,\,theory}$ that is too small for lung deposition (<1 μm) and poor flowability due to the small size (Carr's index >40). Furthermore, the nano-aggregates are poorly reconstituted as reflected in the high S_f/S_i ratio. Nevertheless, at the same nanoparticle to excipient ratio, the S_f/S_i ratio obtained with PVA (≈2.7) is considerably lower than that obtained with mannitol (≈7.8) presented earlier (see Supplementary Data).

Lowering the nanoparticle content to 70% (w/w) in Run 1.1 produces nano-aggregates of larger d_G (≈8–9 μm) as PVA begins to occupy the bulk of the particles, while keeping ρ_{eff} low (≈0.21 g/cm^3). As a result, nano-aggregates having better flowability (Carr's index ≈ 25) and $d_{A,\,theory}$ (≈4 μm) suitable for effective lung deposition are produced at a reasonably high yield (≈65%, w/w). Importantly, the nano-aggregate reconstitution is greatly improved resulting in $S_f/S_i \approx 1.3$, which is again significantly lower than that obtained using mannitol at the same nanoparticle content ($S_f/S_i \approx 7$). The experimental results therefore agree with our postulate that the inclusion of amphiphilic PVA would minimize the inter-nanoparticle fusions attributed to the closer interaction between amphiphilic LC and PVA at the nanoparticle surface compared to that with mannitol.

The nano-aggregates in Run 1.1, however, exhibit poor aerosolization off the PDT as manifested in ED < 10% (w/w). Despite the good flowability during tapping, the nano-aggregates, upon exposure to flowing air, tend to form highly cohesive agglomerates rendering them difficult to be entrained. Lowering the nanoparticle content to 60% (w/w) in Run 2.1 leads to similar observations, i.e. low ED and similar d_G, ρ_{eff}, Carr's index, and S_f/S_i values, albeit a lower production yield (≈38%, w/w). In this regard, our earlier works on SD and SFD of polycaprolactone nanoparticles have demonstrated that leucine, owed to its non hygroscopicity, minimizes nano-aggregate agglomeration resulting in improved aerosolization efficiency (Kho and Hadinoto, 2011). For this reason, leucine is added into the formulation to facilitate the PLGA–LC nano-aggregate aerosolization. The effect of leucine to PVA concentration ratio is investigated next at 70% and 60% (w/w) nanoparticle contents.

At 70% (w/w) nanoparticle content, the inclusion of leucine at 8% (w/w) concentration in Run 1.2 has minimal impacts on the aerosolization, where ED remains low at <10% (w/w). In fact, nano-aggregates having largely similar characteristics (i.e. d_G, ρ_{eff}, flowability) as those in Run 1.1 are produced. Importantly, the leucine inclusion has adverse effects on the production yield, which decreases to ≈21% (w/w), and on the S_f/S_i ratio, which increases to ≈1.7, from 65% (w/w) and 1.3, respectively, in the absence of leucine. The higher S_f/S_i ratio is not unexpected as the presence of hydrophobic leucine reduces particle wetting hence retarding dissolution of the "interstitial bridges". A further increase in the leucine concentration is therefore not pursued as it will lead to even higher S_f/S_i values.

At 60% (w/w) nanoparticle content, the presence of leucine at 10% (w/w) concentration in Run 2.2 is able to increase ED to a respectable value of ≈62% (w/w). The FPF, however, remains low <5% (w/w) indicating that the nano-aggregates are aerosolized off the inhaler in the form of agglomerates (CI ≈ 2.9), such that they predominantly end up in the PS, which results in MMAD ≈7.8 μm too large for effective lung deposition. In terms of the physical characteristics, the nano-aggregates produced are slightly smaller at $d_G \approx 5$–6 μm, but with minimal variations in ρ_{eff}, $d_{A,\,theory}$, yield, and flowability. Not unexpectedly, the S_f/S_i ratio is increased slightly to ≈1.5 compared to that without leucine.

In an attempt to increase the FPF, the leucine concentration is increased to 30% (w/w), while lowering the PVA concentration to 10% (w/w) in Run 2.3. A higher FPF (≈10%, w/w) resulting in MMAD ≈6.8 μm and CI ≈ 2.0, which remains far from ideal, is obtained, but with a lower ED ≈51% (w/w). The S_f/S_i ratio expectedly increases further to ≈1.8. Again, relatively minimal variations are observed in d_G, ρ_{eff}, and $d_{A,\,theory}$. In contrast, the yield is reduced considerably to 16% (w/w) as a larger amount of particles are observed to adhere to the cyclone separator walls, which indicates an increased presence of fine particles that cannot be recovered, hence the lower yield. For the recovered particles, they exhibit lower flowability (Carr's index ≈37), which may explain for the lower ED.

A higher FPF can be obtained by increasing the leucine concentration further, however, it will lead to even higher S_f/S_i and further reductions in ED, yield, and flowability rendering it an infeasible option. In order to increase the leucine concentration further without adversely affecting the other characteristics of the nano-aggregates, the nanoparticle concentration is reduced to 50% (w/w) in Runs 3.1 and 3.2. Theoretically, by lowering the nanoparticle concentration to 50% (w/w), a lower amount of PVA is needed to achieve effective reconstitution of the nano-aggregates, such that a higher leucine to PVA ratio, which would improve the FPF, can be afforded without jeopardizing the nano-aggregate reconstitution.

Previously, at 60% (w/w) nanoparticle concentration, a minimum leucine to PVA ratio equal to 1:3 (Run 2.2) is needed to obtain reconstitutable nano-aggregates ($S_f/S_i \approx 1.5$). In contrast, at 50% (w/w) nanoparticle concentration, higher leucine to PVA ratios of 2.3:1 in Run 3.1 and 4:1 in Run 3.2 can produce highly reconstitutable nano-aggregates, which is reflected in their low S_f/S_i ratios (≈1.1–1.2). The size distributions of the reconstituted nanoparticles from Runs 3.1 and 3.2 are shown in Fig. 3A to be minimally varied from the raw nanoparticle size, except for the presence of a minute peak in the ≈100 nm range, which is likely contributed by fragments of the nanoparticles or the excipients.

Importantly, the nano-aggregates in Runs 3.1 and 3.2 remain to possess d_G and $d_{A,\,theory}$ in the desirable range despite the high leucine content. On this note, the higher leucine to PVA ratio in Run 3.2 results in a larger volume-averaged d_G than that in Run 3.1 due to the existence of a secondary peak at ≈18 μmin addition to the primary peak at ≈10 μm (Fig. 3B), whereas the nano-aggregates in Run 3.1 exhibit a highly uniform size distribution with a monomodal peak at ≈8 μm. SEM images of the nano-aggregates indicate that they have a dimpled spherical shape (Fig. 4A) and a hollow morphology (Fig. 4B) resulting in the low ρ_{eff}.

Similar to the observations in Run 2.3, spray drying at high leucine to PVA ratios in Runs 3.1 and 3.2 results in (1) low production yields around 23–24% (w/w), which are again due to increased particle adhesion in the cyclone separator walls and (2) less than ideal flowability (Carr's index ≈33–38). As a result of the less than ideal flowability, Runs 3.1 and 3.2 fail to significantly improve the ED, which remains to be below 70% (w/w). In terms of the FPF, the leucine to PVA ratio equal to 4:1 in Run 3.2 improves the FPF significantly to ≈23% (w/w), therefore approaching the typical FPF obtained in commercial DPI products. In contrast, the lower leucine to PVA ratio in Run 3.1 has a minimal impact on the FPF (≈12% w/w).

The NGI deposition patterns of the nano-aggregates in Fig. 5 indicate that a significant fraction of the aerosolized particles from

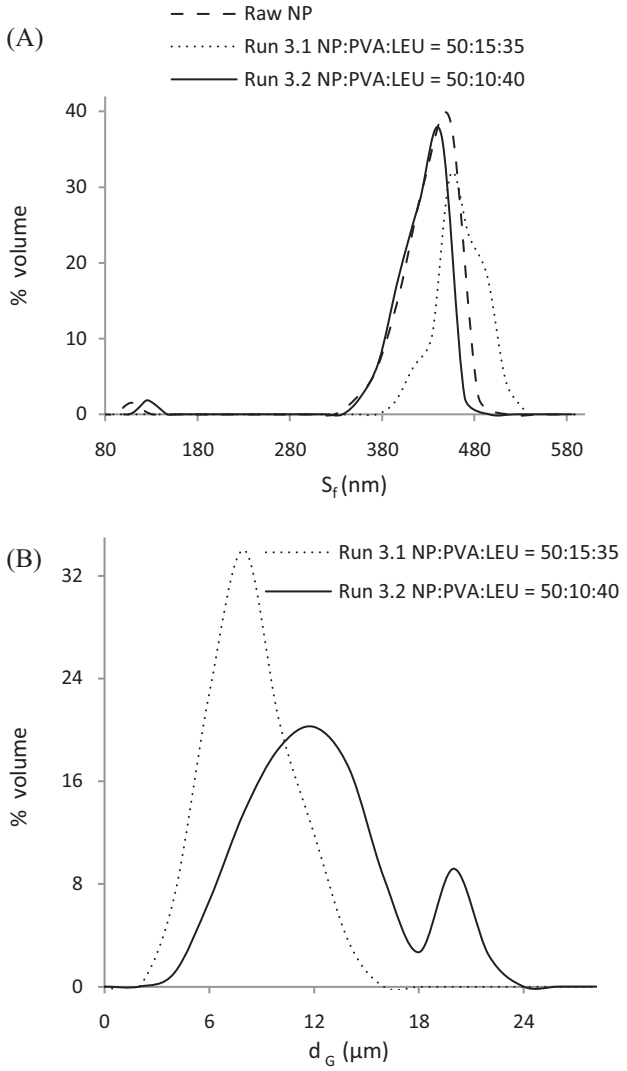

Fig. 3. (A) Nanoparticle size distributions after aqueous reconstitution of the nano-aggregates and (B) geometric size distribution of the spray-dried PLGA–LC nano-aggregates from Runs 3.1 and 3.2.

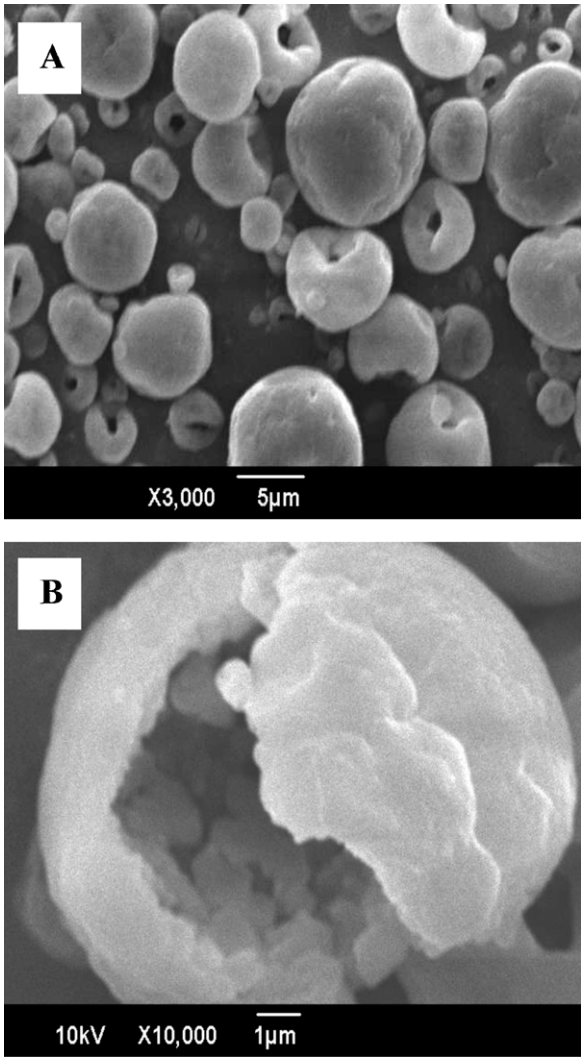

Fig. 4. SEM images of the spray-dried PLGA–LC nano-aggregates from Run 3.1 (A) general particle population and (B) a closer look reveals the hollow morphology reflected in the low ρ_{eff}.

Run 3.1 end up in the PS, which signifies that the particles remain agglomerated in their aerosolized state, as manifested in the high CI (≈2.5), resulting in the low FPF. The fraction of the aerosolized particles that end up in the PS is reduced considerably in Run 3.2 as the increased presence of leucine results in better agglomerate dispersion reflected in the lower CI of ≈1.4. The NGI deposition patterns, however, indicate that a majority of the particles in Run 3.2 deposit in stage 1, instead of in stages 2 or 3 that have lower cut-off d_A, resulting in high MMAD (≈6.6 μm). Therefore, despite the greatly improved FPF, the nano-aggregates produced in Run 3.2 would still exhibit low particle deposition in the lung.

In summary, the spray-dried PLGA–LC nano-aggregates remain to exhibit far from ideal aerosolization characteristics in terms of ED (<70%, w/w) and MMAD (>5 μm), despite spray drying at 1:1 nanoparticle to excipient ratio and at a high leucine to PVA ratio. The optimal formulation (i.e. Run 3.2) manages to increase the FPF to a respectable value of ≈23%, but at the expense of the production yield (≈20% w/w) and flowability (Carr's index >25). Decreasing the nanoparticle content to below 50% (w/w) may enable the leucine to PVA ratio to be increased beyond 4:1 to decrease the MMAD, without any adverse effect on the aqueous reconstitution. However, it will likely lead to even lower ED and production yield. Furthermore, having lower nanoparticle contents is impractical considering that

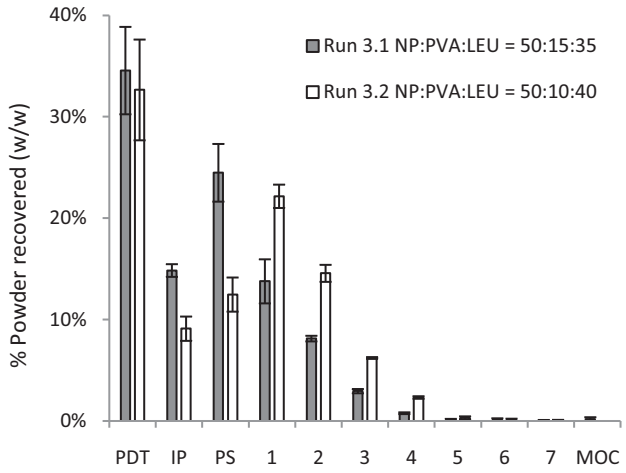

Fig. 5. NGI deposition patterns of the spray-dried PLGA–LC nano-aggregates from Runs 3.1 and 3.2.

Table 3
SFD: nano-aggregate physical and aerosolization characteristics with mannitol and leucine as the excipients at 60% (w/w) nanoparticle content.

LEU: Mannitol	d_G (μm)	ρ_{eff} (g/cm^3)	$d_{A,\ theory}$ (μm)	Yield (%, w/w)	Carr's index	S_f/S_i	ED (%, w/w)	FPF (%, w/w)	MMAD (μm)	CI
1:1.7	18	0.035	3.4	22	17	2.9	90	6	9.8	2.9
1:1	18	0.039	3.6	16	23	3.4	87	5	10.6	2.9

the typical drug loading in polymeric nano-carriers is less than 10% (w/w), such that the nanoparticle to excipient ratio must be kept as high as possible. Therefore, an alternative method to spray drying is investigated next.

3.3. Spray-freeze-dried lipid–polymer hybrid nano-aggregates

The SFD experiments are started at 60% (w/w) nanoparticle content for both the mannitol and PVA formulations based on the SD results, where higher nanoparticle contents lead to less than optimal nano-aggregate reconstitution. Also from the SD results, leucine is added in both mannitol and PVA formulations to facilitate nano-aggregate aerosolization.

3.3.1. Using mannitol as excipient

At 60% (w/w) nanoparticle content and leucine to mannitol ratio equal to 1:1.7, the spray-freeze-dried PLGA–LC nano-aggregates possess all the desirable physical characteristics for pulmonary delivery (Table 3), where large d_G (≈18 μm), low ρ_{eff} (≈0.04 g/cm^3), resulting in $d_{A,\ theory}$ ≈ 3–4 μm, and good flowability (Carr's index <25) are observed. The production yield, however, is rather low at ≈22% (w/w). Importantly, similar to the findings in the SD experiment using mannitol and leucine as the excipients, the spray-freeze-dried nano-aggregates are poorly reconstitutable (S_f/S_i ≈ 2.9), despite the high excipient content. Unlike their spray-dried counterparts, however, the spray-freeze-dried nano-aggregates are readily aerosolized off the PDT owed to their good flowability and low density resulting in ED ≈90% (w/w). The FPF, however, is low at ≈6% (w/w) suggesting that the nano-aggregates are aerosolized in the form of agglomerates (MMAD ≈10 μm and CI ≈ 2.9).

Increasing the leucine to mannitol concentration ratio to 1:1 does not improve the FPF and leads to a higher S_f/S_i ratio (≈3.4) as expected, while it has relatively minimal impacts on the other characteristics (e.g. d_G, ρ_{eff}, Carr's index, ED). The results of the SFD experiments therefore reaffirm the findings of the SD experiments that mannitol is not suitable to function as the "interstitial bridges" of the hybrid nanoparticle aggregates. Even though the nano-aggregate reconstitution can possibly be improved by lowering the nanoparticle content, a large amount of mannitol will likely be needed considering that presently S_f/S_i ratio is much larger than one. Importantly, the high requirement in the mannitol amount would limit the amount of leucine that can be added, therefore rendering improvement in the FPF becomes unlikely. For this reason, we focus on the use of PVA as the excipient in the SFD formulation.

3.3.2. Using PVA as excipient

The physical and aerosolization characteristics of the spray-freeze-dried PLGA–LC nano-aggregates as a function of the leucine to PVA concentration ratio are presented in Tables 4 and 5, respectively. At 60% (w/w) nanoparticle content and leucine to PVA ratio equal to 1:1 (Run A1), the nano-aggregates produced are highly similar in terms of their physical characteristics (e.g. d_G, ρ_{eff}, yield, Carr's index) to those produced with mannitol at exactly the same conditions. One exception is in their S_f/S_i ratios, where replacing mannitol with PVA results in highly reconstitutable nano-aggregates (S_f/S_i ≈ 1). This result therefore further confirms that PVA is the more appropriate excipient for DPI formulations of hybrid nanoparticles involving lecithin.

In terms of the aerosolization characteristics, the nano-aggregates from Run A1 are readily aerosolized off the PDT (ED ≈ 85%, w/w), but a majority of the particles end up in the PS (data not shown) as reflected in the FPF being less than 5% (w/w). To improve the FPF, the leucine to PVA ratio is increased to 1.7:1 in Run A.2 improving the FPF to ≈15% (w/w), while variations in the other characteristics are statistically insignificant, except for the yield that is more than doubled to ≈47% (w/w). The MMAD, however, is still too high at ≈7.6 μm, where the high CI (≈3.0) suggests that the aerosolized particles are agglomerated upon entering the NGI.

Increasing the leucine to PVA ratio further to 3:1 in Run A.3, which should help dispersing the aerosolized particles better, only increases the FPF slightly to ≈19% (w/w) and lowers the MMAD to ≈6.4 μm. While the high leucine to PVA ratio in Run A.3 has relatively insignificant impacts on the nano-aggregate physical characteristics, the aqueous reconstitution deteriorates due to poorer particle wetting at high leucine concentrations resulting in S_f/S_i ≈ 1.9. Therefore, the only means to improve the MMAD is by lowering the nanoparticle content below 60% (w/w).

At 50% (w/w) nanoparticle content, the nano-aggregates remain highly reconstitutable (S_f/S_i ≈ 1.0) at leucine to PVA concentration ratio equal to 2.3:1 in Run B.1, whereas at 60% (w/w) nanoparticle content, the maximum leucine to PVA concentration ratio for effective reconstitution is 1.7:1 (Run A.2). Excluding the aqueous reconstitution, nano-aggregates of relatively similar characteristics (e.g. d_G, ρ_{eff}, $d_{A,\ theory}$, yield, and Carr's index) are produced at 50 and 60% (w/w) nanoparticle contents. Nevertheless, the size distribution of the nanoparticles from Run B.1 after reconstitution in Fig. 6 suggests that the reconstituted nanoparticles are slightly smaller (S_f ≈ 350 nm), which is likely contributed by the lyophilization step. Furthermore, a secondary peak around 100 nm appears after reconstitution similar to the spray-dried nano-aggregates due to presence of fragments.

SEM image of the nano-aggregates from Run B.1 in Fig. 7A denote their spherical shape and highly porous structure, which is inherent in spray-freeze-dried powders attributed to interstitial sublimation of the ice crystals. A closer look at the nano-aggregate

Table 4
SFD: nano-aggregate physical characteristics with PVA and leucine as the excipients.

Run	NP (%, w/w)	PVA (%, w/w)	LEU (%, w/w)	d_G (μm)	ρ_{eff} (g/cm^3)	$d_{A,\ theory}$ (μm)	Yield (%, w/w)	Carr's index	S_f/S_i
A.1	60	20	20	17	0.06	4.1	20	20	1.0
A.2		15	25	15	0.03	2.6	47	15	1.1
A.3		10	30	17	0.02	2.3	34	18	1.9
B.1	50	15	35	15	0.03	2.5	33	17	1.0
B.2		10	40	17	0.02	2.2	26	21	1.2

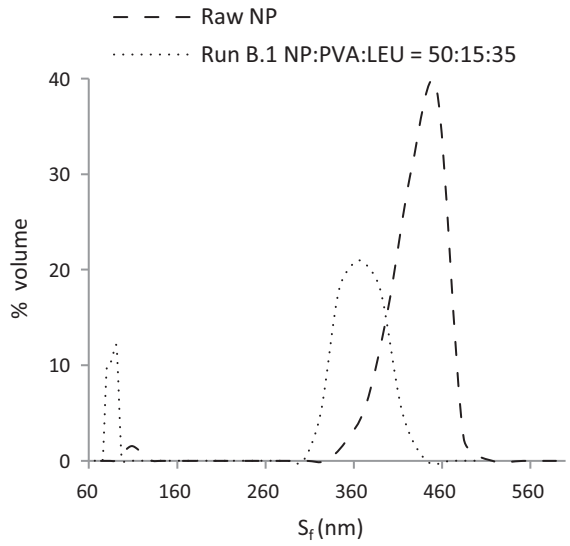

Fig. 6. Nanoparticle size distribution after aqueous reconstitution of the nano-aggregates of Run B.1.

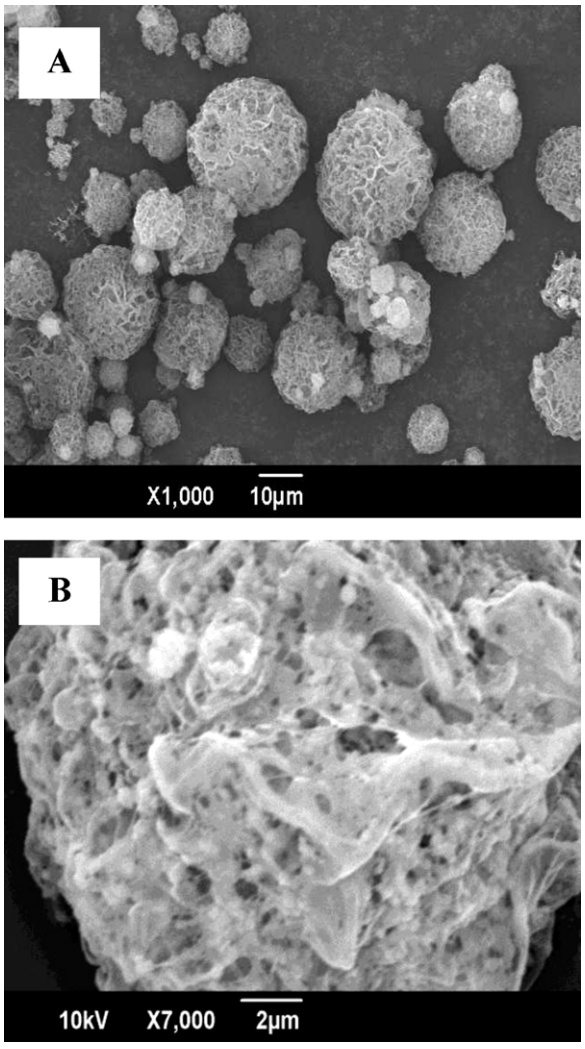

Fig. 7. SEM images of the spray-freeze-dried PLGA–LC nano-aggregates from Run B.1 (A) general particle population and (B) a closer look reveals the porous morphology reflected in the low ρ_{eff}.

Table 5
SFD: nano-aggregate aerosolization characteristics with PVA and leucine as the excipients.

Run	ED (%, w/w)	FPF (%, w/w)	MMAD (μm)	CI
A.1	85	2	14.2	3.4
A.2	87	15	7.6	3.0
A.3	84	19	6.4	2.8
B.1	92	26	5.6	2.2
B.2	92	26	5.8	2.7

surface in Fig. 7B reveals that the PLGA–LC nanoparticles are physically dispersed in the porous matrix of PVA. The spray-freeze-dried nano-aggregates are considerably larger and lighter than their spray-dried counterparts (i.e. 18 versus 9 μm and 0.03 versus 0.3 g/cm^3, respectively), however, the spray-freeze-dried powders exhibit a wider range of size distribution as shown in Fig. 8A.

By having a higher leucine to PVA ratio in Run B.1, the FPF is increased to ≈26% (w/w) and ED remains high at ≈92% (w/w) resulting in MMAD ≈5.6 μm, which are closer to the typical ED, FPF, and MMAD values obtained in commercial DPI products. The NGI deposition patterns of the nano-aggregates are presented in Fig. 8B showing that a significant fraction of the particles are recovered in stages 2 and 3. The CI, however, remains high at ≈2.2 suggesting that agglomeration of the aerosolized particles is still prevalent despite the increased presence of leucine. In an attempt to reduce the MMAD and in turn CI, the leucine to PVA ratio is increased to 4:1

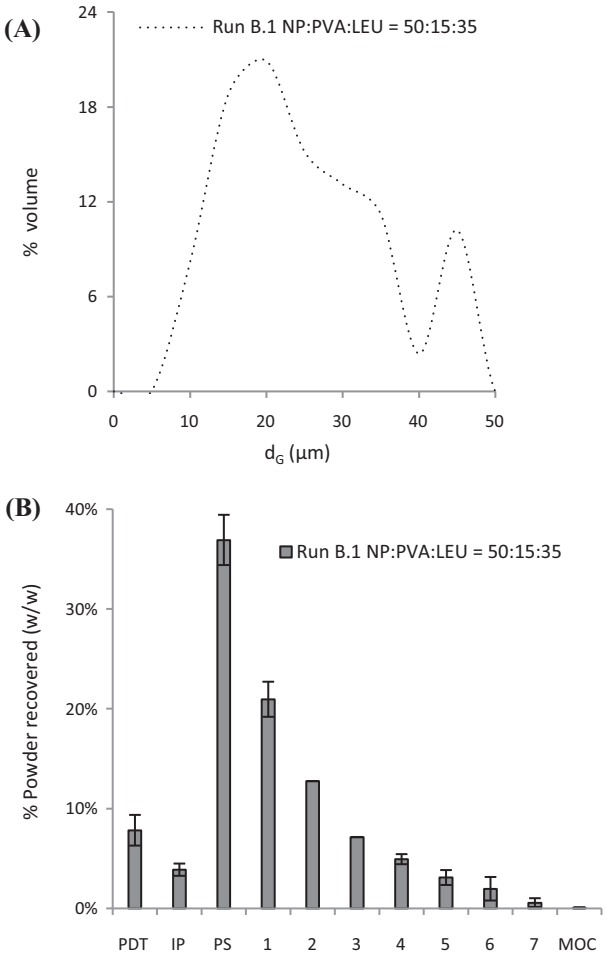

Fig. 8. (A) geometric size distribution and (B) NGI deposition patterns of the spray-freeze-dried PLGA–LC nano-aggregates from Run B.1.

in Run B.2. The results, however, indicate that the higher leucine to PVA concentration ratio in Run B.2 does not lead to improvement in the aerosolization characteristics.

In summary, SFD of the PLGA–LC nanoparticles at 50% (w/w) nanoparticle content and leucine to PVA ratio equal to 2.3:1 is capable of producing nano-aggregates having the physical and aerosolization characteristics ideal for inhaled delivery to the lung. Nevertheless, the current production yield at 33% (w/w) leaves much room for improvement. Unlike the SD yield, which is influenced by many parameters (e.g. temperature, flowrate, particle collection), the SFD yield is governed by the spray-freezing step, where the final amount of the product depends on how much of the sprayed droplet is lost on the walls of the liquid nitrogen vessel. Therefore, we believe that the SFD yield can be increased by simply using a wider liquid nitrogen container. Comparing the optimal SFD formulation (i.e. Run B.1) with that of the SD formulation (i.e. Run 3.2), SFD is found to be vastly superior to SD for DPI formulation of hybrid nanoparticles as it produces nano-aggregates of larger d_G resulting in easier physical handling, higher yield and reconstitutibility, better flowability, as well as higher ED, FPF, and lower MMAD.

4. Conclusion

Inhalable dry-powder form of drug-loaded lipid–polymer hybrid nanoparticles has been successfully produced by SD and SFD in the form of micro-scale aggregates of the nanoparticles. Hollow dimpled spherical nano-aggregates are produced by SD, whereas SFD produces large spherical porous nano-aggregates. For both SD and SFD, PVA has been found to be more effective than mannitol in facilitating the nano-aggregate reconstitution. In addition, the inclusion of leucine is crucial to achieve effective aerosolization of the nano-aggregates. Overall, nano-aggregates produced by SFD exhibit superior characteristics compared to those produced by SD in terms of size, yield, flowability, aqueous reconstitutibility, and aerosolization efficiency. One caveat about SFD is that the hybrid nanoparticles exhibit a slight change in size after reconstitution from the nano-aggregates, which is believed to occur in the lyophilization step. A study on the effect of the lyophilization condition on the reconstituted nanoparticle size is currently ongoing in our laboratory.

Acknowledgments

The authors gratefully acknowledge the funding from Ministry of Education of Singapore AcRF Tier I Grant No. RG 76/10. We also wish to acknowledge the funding support for this project from Nanyang Technological University under the Undergraduate Research Experience on CAmpus (URECA) programme.

Appendix A. Supplementary data

Supplementary data associated with this article can be found, in the online version, at doi:10.1016/j.ijpharm.2011.12.045.

References

Bershteyn, A., Chaparro, J., Yau, R., Kim, M., Reinherz, E., Ferreira-Moita, L., Irvine, D.J., 2008. Polymer-supported lipid shells, onions, and flowers. Soft Matter 4, 1787–1791.
Cheow, W.S., Hadinoto, K., 2011. Factors affecting drug encapsulation and stability of lipid–polymer hybrid nanoparticles. Colloids Surf. B: Biointerfaces 85, 214–220.
Cheow, W.S., Ng, M.L.L., Kho, K., Hadinoto, K., 2011. Spray-freeze-drying production of thermally sensitive polymeric nanoparticle aggregates for inhaled drug delivery: effect of freeze-drying adjuvants. Int. J. Pharm. 404, 289–300.
D'Aurizio, E., van Nostrum, C.F., van Steenbergen, M.J., Sozio, P., Siepmann, F., Siepmann, J., Hennink, W.E., Di Stefano, A., 2011. Preparation and characterization of poly(lactic-co-glycolic acid) microspheres loaded with a labile antiparkinson prodrug. Int. J. Pharm. 409, 289–296.
Finley, J.H., 1961. Spectrophotometric determination of polyvinyl alcohol in paper coatings. Anal. Chem. 33, 1925–1927.
Hu, C.-M.J., Kaushal, S., Cao, H.S.T., Aryal, S., Sartor, M., Esener, S., Bouvet, M., Zhang, L., 2010. Half-antibody functionalized lipid–polymer hybrid nanoparticles for targeted drug delivery to carcinoembryonic antigen presenting pancreatic cancer cells. Mol. Pharmacol. 7, 914–920.
Jensen, D.M.K., Cun, D., Maltesen, M.J., Frokjaer, S., Nielsen, H.M., Foged, C., 2010. Spray drying of siRNA-containing PLGA nanoparticles intended for inhalation. J. Control. Release 142, 138–145.
Kho, K., Hadinoto, K., 2010. Aqueous re-dispersibility characterization of spray-dried hollow spherical silica nano-aggregates. Powder Technol. 198, 354–363.
Kho, K., Hadinoto, K., 2011. Optimizing aerosolization efficiency of dry-powder aggregates of thermally-sensitive polymeric nanoparticles produced by spray-freeze-drying. Powder Technol. 214, 169–176.
Louey, M.D., Van Oort, M., Hickey, A.J., 2006. Standardized entrainment tubes for the evaluation of pharmaceutical dry powder dispersion. J. Aerosol Sci. 37, 1520–1531.
Ohashi, K., Kabasawa, T., Ozeki, T., Okada, H., 2009. One-step preparation of rifampicin/poly(lactic-co-glycolic acid) nanoparticle-containing mannitol microspheres using a four-fluid nozzle spray drier for inhalation therapy of tuberculosis. J. Control. Release 135, 19–24.
Rogueda, P.G.A., Traini, D., 2007. The nanoscale in pulmonary delivery. Part 1: deposition, fate, toxicology and effects. Expert Opin. Drug Deliv. 4, 595–606.
Salama, R., Hoe, S., Chan, H.K., Traini, D., Young, P.M., 2008. Preparation and characterisation of controlled release co-spray dried drug-polymer microparticles for inhalation 1: influence of polymer concentration on physical and in vitro characteristics. Eur. J. Pharm. Biopharm. 69, 486–495.
Sanchez, J., 1998. Colorimetric assay of alditols in complex biological samples. J. Agric. Food Chem. 46, 157–160.
Small, D.M., 1967. Phase equilibria and structure of dry and hydrated egg lecithin. J. Lipid Res. 8, 551–557.
Su, X.F., Fricke, J., Kavanagh, D.G., Irvine, D.J., 2011. In vitro and in vivo mRNA delivery using lipid-enveloped ph-responsive polymer nanoparticles. Mol. Pharmacol. 8, 774–787.
Sung, J., Padilla, D., Garcia-Contreras, L., VerBerkmoes, J., Durbin, D., Peloquin, C., Elbert, K., Hickey, A., Edwards, D., 2009. Formulation and pharmacokinetics of self-assembled rifampicin nanoparticle systems for pulmonary delivery. Pharm. Res. 26, 1847–1855.
Takashima, Y., Saito, R., Nakajima, A., Oda, M., Kimura, A., Kanazawa, T., Okada, H., 2007. Spray-drying preparation of microparticles containing cationic PLGA nanospheres as gene carriers for avoiding aggregation of nanospheres. Int. J. Pharm. 343, 262–269.
Tomoda, K., Ohkoshi, T., Hirota, K., Sonavane, G.S., Nakajima, T., Terada, H., Komuro, M., Kitazato, K., Makino, K., 2009. Preparation and properties of inhalable nanocomposite particles for treatment of lung cancer. Colloids Surf. B: Biointerfaces 71, 177–182.
Wade, A., Weller, P.J., 1994. Handbook of Pharmaceutical Excipients, 2nd edition. American Pharmaceutical Association, Washington DC.
Zhang, L., Chan, J.M., Gu, F.X., Rhee, J.-W., Wang, A.Z., Radovic-Moreno, A.F., Alexis, F., Langer, R., Farokhzad, O.C., 2008. Self-assembled lipid–polymer hybrid nanoparticles: a robust drug delivery platform. ACS Nano 2, 1696–1702.
Zheng, Y., Yu, B., Weecharangsan, W., Piao, L., Darby, M., Mao, Y., Koynova, R., Yang, X., Li, H., Xu, S., Lee, L.J., Sugimoto, Y., Brueggemeier, R.W., Lee, R.J., 2010. Transferrin-conjugated lipid-coated PLGA nanoparticles for targeted delivery of aromatase inhibitor 7[alpha]-APTADD to breast cancer cells. Int. J. Pharm. 390, 234–241.